DETERMINING THE RELATIONSHIP BETWEEN SINGLE SCATTERING ALBEDO AND COMPOSITION TO EXPLORE THE CONECENTRATION OF SILICIC MATERIAL WITHIN GRUITHUISEN GAMMA DOME. E. Culley[1], and B. L. Jolliff[1], [1]Department of Earth and Planetary Sciences and the McDonnell Center for the Space Sciences, Washington University in St. Louis, Box 1169, 1 Brookings Drive, Saint Louis, MO 63130, USA. (eculley@wustl.edu)

Introduction: The Gruithuisen Domes, located on the western edge of Imbrium basin, include three distinct domes: Delta, Gamma, and Northwest.

The shape, morphologies, and spectral characteristics of the domes are distinct from both the surrounding highland material and volcanic plains, as well as other lunar mare domes. Analysis of the domes' shape and slope [1], width-height aspect ratios [1], thorium content [2], reflectance and UV absorption [3,4], and internal structure (determined from a region of Gamma dome exposed by a large, fresh crater [1]), suggest that the Gruithuisen domes are nonmare extrusive volcanic structures formed from highly viscous, silica-rich lava [5,6].

The formation mechanism of the Gruithuisen Domes, however, is still debated. One possibility is basaltic underplating, wherein remelting of "fertile" crust generates large volumes of buoyant, silicic magmas that rise to the surface as rhyolitic domes [7]. This model requires a sufficiently large component of fertile material (such as KREEP basalt) that is more silica-rich than the anorthositic primary crust [1]. Extended fractional crystallization of basaltic magma reservoirs could explain the silica-rich composition of the lava, but it fails to account for the significant age difference between the domes and the surrounding mare. [1]. Moreover, fractional crystallization of low-fO_2 lunar magmas typically does not lead to significant silica enrichment in residual melts. Nonetheless, gaining a more detailed understanding of the composition of the domes will help to constrain potential formation scenarios and bolster our understanding of lunar crustal evolution.

This analysis focuses on Gamma dome, which covers ~290 km^3 and rises ~1400 m above the surrounding volcanic plains [1]. Gamma dome has steep slopes (10-20°) [4] and a summit plateau centered at 36.6°N, 40.7°W. Previous analyses have shown that single scattering albedo (SSA) varies linearly with mafic content [3,8]. In this analysis, we determine the SSA of the summit of Gruithuisen Gamma dome and correlate our findings with mafic content, using FeO wt% (calculated from SELENE Multiband Imager [9]) as a proxy. Exploring the nature of the correlation allows us to infer composition and, therefore, concentration of silicic material, at resolutions where compositional data are not available.

Methods and Data: We perform photometric analysis using Narrow Angle Camera (NAC) images from the Lunar Reconnaissance Orbiter Camera (LROC) [10] to determine the SSA of the regolith across the summit of the Gruithuisen Gamma Dome. We use Hapke photometric modeling [11,12] combined with digital terrain models (DTM) [13] to account for local incidence and emission angles at every pixel, allowing us to determine SSA at very high resolutions (2 mpp) (e.g. [3,14]).

Fig. 1 shows the SSA of the full analysis region of Gamma dome. Morphologic units are marked in white,

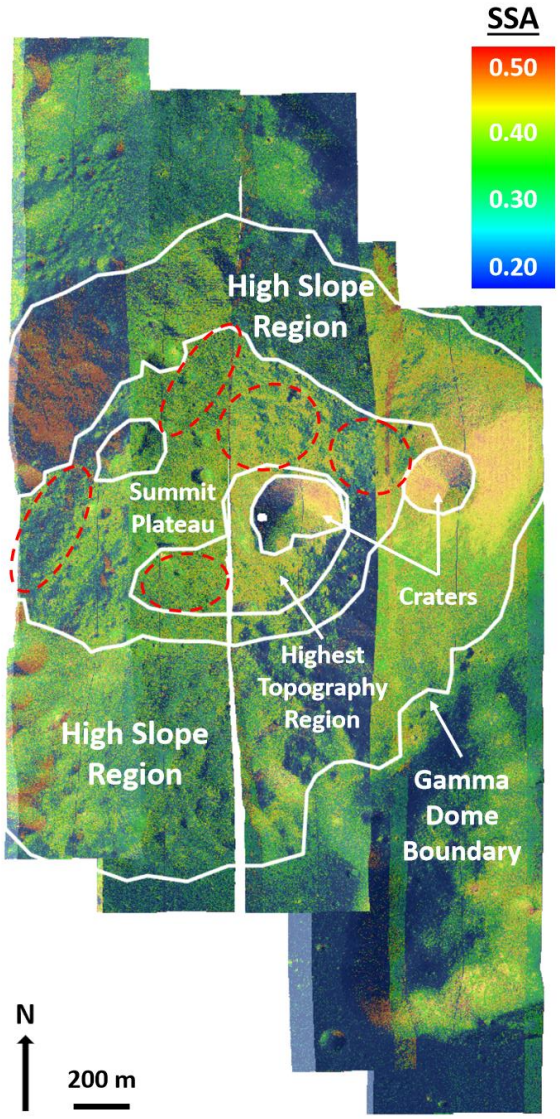

Figure 1. Map of SSA across Gruithuisen Gamma Dome analysis region. White lines indicate morphologic units and dashed red circles indicate regions of interest within the SSA or FeO wt% data sets.

separating the steep-sloped sides of the dome from the summit plateau and craters. To explore the relationship between SSA and FeO wt% for Gamma dome regolith, we sampled regions along the summit that had a range of SSA and FeO values. Previously presented results showed that fresh, immature material typically has a higher SSA than mature regolith and deviates from the linear relationship with mafic content [15]. Thus, in this study, we focus on areas where slope < 10° and OMAT (maturity index computed from data collected by SELENE) < 0.24 [9].

Additionally, we focus on regions of interest (ROI), dashed in red in Fig. 1, where either SSA or FeO content appear to be consistent within the region.

Finally, we conduct a preliminary sampling of the SSA and FeO wt% of the northwestern highland material and southern mare material to explore how these compositions might deviate from the correlation of the Gamma dome summit plateau material.

Results and Discussion: Fig. 2 shows the correlation between single scattering albedo and FeO wt% determined in this analysis. The blue dots show each subregion we sampled while the red triangles average these subregions based on the ROI locations highlighted in Fig. 1. The green line shows the best fit for both data sets, with $R^2 = 0.80$.

The range of values determined by [3] are represented by the shaded region in the center of Fig. 2. This study sampled more data across a larger area, giving a larger spread in the data than Clegg-Watkins et al. (2017) observed. However, nearly all of the ROI averages fall within the same range, showing consistency between the two studies.

To better understand the range in SSA across Gamma dome, we measure the highland material to the northwest and mare material to the southeast, shown in Fig. 2 by the brown and purple open diamonds, respectively. These areas both exhibit higher SSA than Gamma dome areas would at the same FeO wt%. The highlands data are comparable to data found in this study as well as within the region determined by Clegg-Watkins et al. (2017). Conversely, the mare data are isolated from the data set, possessing noticeably higher FeO content and lower SSA than most of the Gamma dome data. Thus, the spread in the Gamma dome SSA range could indicate mixing with nearby highlands material or the presence of intermediate silicic material different from either highlands or mare source.

Focusing on the regions of interest, most of the data flank the best fit line. The data point that deviates furthest, located above the best fit line, corresponds to the area of highest topography near the large central crater. The elevated SSA values in this average could reflect the presence of more immature ejecta deposited during crater formation rather than composition of the region.

Conclusions: In this study, we explored the concentration of silicic material as a function of FeO wt% with SSA across the summit of Gruithuisen Gamma dome. We find a relatively tight correlation, including values that agree with previous findings [3]. The highest albedo, lowest FeO data are the most consistent with known silicic materials in the Apollo samples. Those with FeO >6 wt% reflect mixing with a higher FeO source, either exogenous (ejecta from craters into surrounding more mafic materials) or endogenous (such as complementary mafic material of the alkali suite such as monzogabbro).

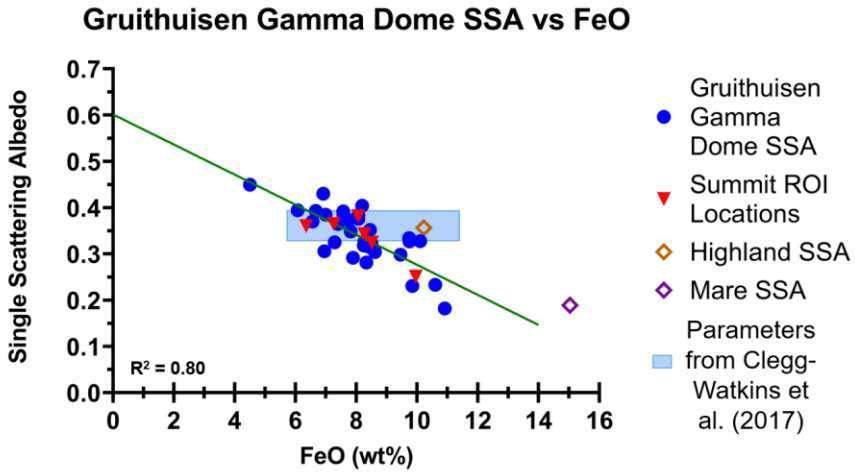

Figure 2. Relationship between SSA and FeO wt% across Gruithuisen Gamma Dome Summit. Blue points indicate all data collected; red points highlight averages of regions of interest. Open diamonds represent average data for highland and mare material. Shaded region corresponds to data from [3]

Acknowledgments: We thank NASA for support of the LRO extended mission and for the hard work of the LRO & LROC Operations Teams. Additional thanks to the LROC Photometry Group and colleagues at ASU for production of NAC DTMs.

References: [1] Ivanov M. et al. (2016) *Icarus* **273**, 262-283. [2] Hagerty J. et al. (2006) *JGR* **111**, E06002. [3] Clegg-Watkins R. et al. (2017) *Icarus* **285**, 169-184. [4] Braden S. et al. (2010) *LPSC* **41**, #2677. [5] Head J. and McCord T. (1978) *Science* **199**, 1433-1436. [6] Chevrel S. et al. (1999) *JGR* **104**, 16515-16529. [7] Glotch T. et al. (2010) *Science* **329**, 1510-1513. [8] Schonwald A. et al. (2019) *LPSC* **50**, #1239. [9] Lucey P. et al. (2000) *JGR* **105**, 20377-20386. [10] Robinson M. et al. (2010) *Space Sci Rev* **150**, 81-124. [11] Hapke B. (2012a) *Icarus*, **221** (2), 1079-1083. [12] Hapke B. (2012b) *Theory of Reflectance and Emittance Spectroscopy* (2nd Ed). [13] Henriksen M. (2017) *Icarus* **283**, 122-137. [14] Hahn T. (2019) *LPSC* **50**, #1976. [15] Jolliff B. et al. (2020) *LPSC* **51**, #2362.